Determination of the complex frequencies for the normal modes below 1mHz after the 2010 Maule and 2011 Tohoku earthquakes

Hao Ding[1], WenBin Shen[1,2,*]

[1] *Wuhan University, Department of Geophysics, School of Geodesy and Geomatics, Key Laboratory of Geospace Environment and Geodesy of the Ministry of Education, Wuhan, China*

[2] *State Key Laboratory of Information Engineering in Surveying, Mapping and Remote Sensing, China*

Article history
Received August 18, 2013; accepted November 21, 2013.
Subject classification:
Normal modes, Splitting, Frequency, Quality factor Q.

ABSTRACT

Based upon SG (superconducting gravimeter) records, the autoregressive method proposed by Chao and Gilbert [1980] is used to determine the frequencies of the singlets of seven spheroidal modes ($_0S_2$, $_2S_1$, $_0S_3$, $_0S_4$, $_1S_2$, $_0S_0$, and $_3S_1$) and the degenerate frequencies of three toroidal modes ($_0T_2$, $_0T_3$, and $_0T_4$) below 1 mHz after two recent huge earthquakes, the 2010 Mw8.8 Maule earthquake and the 2011 Mw9.1 Tohoku earthquake. The corresponding quality factors Qs *are also determined for those modes, of which the* Qs *of the five singlets of $_1S_2$ and the five singlets (*m=0, m=±2, *and* m=±3*) of $_0S_4$ are estimated for the first time using the SG observations. The singlet* m=0 *of $_3S_1$ is clearly observed from the power spectra of the SG time series without using other special spectral analysis methods or special time series of polar station records. In addition, the splitting width ratio* R *of $_3S_1$ is 0.99, and consequently we conclude that $_3S_1$ is normally split. The frequencies and* Qs *of the modes below 1mHz can contribute to refining the 3D density and attenuation models of the Earth.*

1. Introduction

The normal modes below 1mHz are very sensitive to density heterogeneities of the Earth, and precise determination of the splitting frequencies of these modes can provide further information to constrain the 3D models, especially the core and mantle density distribution and structures. For instance, the observations of the splitting of $_0S_2$, $_0S_3$, and $_0S_4$ may provide further information to constrain the mantle structure [Okal 1978, He and Tromp 1996, Roult et al. 2010]; the observations of the splitting of $_2S_1$ may help to constrain the outer core and mantle models [Rosat et al. 2003]; the observations of $_1S_2$ may provide additional constraints on the 3D models, especially the mantle structure [Roult et al. 2010, Deuss et al. 2011]; and the observations of $_3S_1$ may constrain the Earth's density and the core structure [Chao and Gilbert 1980, He and Tromp 1996]. In addition, determining the quality factors *Q*s of those modes may also help to improve the knowledge of the 3D attenuation model of the Earth [Roult et al. 2006].

Numerous studies have dedicated to obtaining the frequencies of all of the singlets of the modes below 1mHz. All of the singlets of $_0S_2$ and $_0S_3$ were completely observed by Buland et al. [1979] using seismic datasets from the International Deployment of Accerometers (IDA) network, and the triplet of $_2S_1$ was first observed by Rosat et al. [2003] based on five SG records. The triplet of $_3S_1$ was first observed by Chao and Gilbert [1980] using seismic datasets from IDA network. The above mentioned four modes and the modes $_1S_2$, $_0S_4$, $_0S_5$ have been extensively investigated by other scholars [e.g., Ritzwoller et al. 1986, Giardini et al. 1988, Widmer-Schnidrig et al. 1992a, Resovsky and Ritzwoller 1998, Hu et al. 2006, Widmer-Schnidrig and Laske 2007, Roult et al. 2010, Deuss et al. 2011, Shen and Wu 2012, Ding and Shen 2013].

Except for the mode $_0S_0$, only few studies concerned about the quality factors *Q*s of the whole set of the singlets of those modes. The *Q* of $_0S_0$ was determined by various authors [e.g., Sailor and Dziewonski 1978, Buland et al. 1979, Chao and Gilbert 1980, Riedesel et al. 1980, Dziewonski and Anderson 1981, Roult et al. 2006, Rosat et al. 2007, Xu et al. 2008, Abd El-Gelil et al. 2010, Zábranová et al. 2012]. The *Q*s of all of the five singlets of $_0S_2$ were first estimated by Tanimoto [1990], and then re-estimated by Roult et al. [2006], Rosat et al. [2008] and Abd El-Gelil et al. [2010]. The *Q*s of all of the singlets of $_0S_3$ and $_2S_1$ were first estimated by Roult et al. [2006]. Rosat et al. [2008] and Abd El-Gelil et al. [2010] further provided the refined

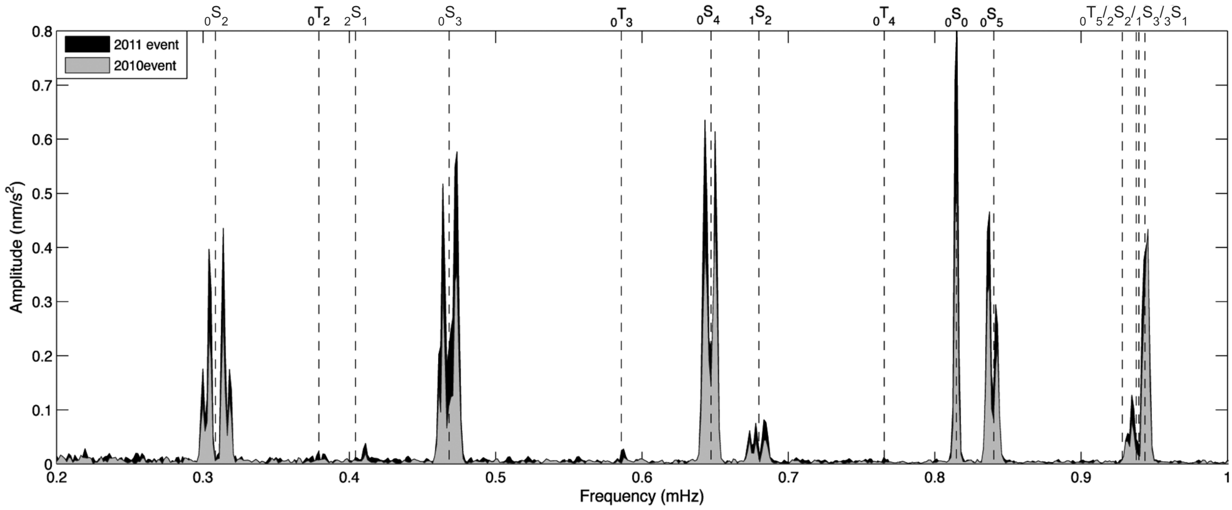

Figure 1. The amplitude spectra of the residual gravity sequences from CB station after the 2010 Maule event (gray area) and 2011 Tohoku event (black area), both of the sequences starting 5h after the earthquake with a length of 200h.

measurements of Qs of the seven singlets of $_0S_3$. As for the toroidal modes below 1mHz, the degenerate frequencies of $_0T_2$, $_0T_3$ and $_0T_4$, and Qs of $_0T_3$ and $_0T_4$ have been determined [e.g., Widmer-Schnidrig et al. 1992b, Tromp and Zanzerkia 1995, Hu et al. 2006, Abd El-Gelil et al. 2010], and Roult et al. [2010] even have determined the five split frequencies of $_0T_2$. Due to the fact that the frequencies of $_0T_5$, $_2S_2$ and $_1S_3$ are very close to each other, it is hard to distinguish them from the spectra of the chosen time series. Since the singlets m=0 of $_2S_1$ and $_3S_1$ are difficult to clearly observe to date, the main purpose of this paper is to re-determine or newly determine the frequencies and Qs of the whole set of the singlets of the modes $_0S_0$, $_0S_2$, $_1S_2$, $_2S_1$, $_0S_3$, $_3S_1$, $_0S_4$, $_0T_2$, $_0T_3$, and $_0T_4$.

Since SGs deployed in the frame of the Global Geodynamics Project (GGP) can outmatch the best seismometers in the frequency band below 1mHz [e.g., Widmer-Schnidrig 2003], and since the 2010 Mw8.8 Maule earthquake and the 2011 Mw9.1 Tohoku earthquake have strongly excited the normal modes (see Figure 1), SG records after the two events are used to determine the relevant frequencies and Qs. In this study, after the 2010 event, we use 13 SG records from different stations, listing as Apache Point (AP), Bad Homburg (BH), Schiltach (BF, the Black Forest Observatory), Cantley (CA), Canberra (CB), Membach (MB), Medicina (MC), Moxa (MO), Ny-Alesund (NY), Pecny (PE), Sutherland (SU), Strasbourg (ST), and Wettzell (WE). After the 2011 event, we use the records from 13 SG stations, listing as AP, BF, BH, CB, Conrad (CO), MB, MC, MO, NY, PE, ST, Concepcion (TC), and WE. According to Dahlen [1982], in general cases, the optimum record length should be about 1.1Q-cycle of the modes. However, in order to obtain a sufficient frequency resolution, for each mode, the selection of the data length needs not following that criterion [e.g., Rosat et al. 2005, Roult et al. 2010]. Because the noise levels of those SG stations are different from each other [Rosat and Hinderer 2011], we choose different groups of records for different modes; and because different events may excite different amplitudes even for the same mode, we choose different groups of records for a given mode (see details in Section 3).We note that, in this study, the sampling interval of all records is 1min, and for each of the target modes except for $_3S_1$, all records start 5h after the earthquakes; as for $_3S_1$, data sets with a 50h later starting point after the earthquake are used to weaken the interference of $_1S_3$ [Masters and Gilbert 1983]. For each of the chosen records, after removing the tidal and local atmospheric pressure effects, we obtain the corresponding residual gravity time series for further use.

2. The estimate method for frequencies and Qs

For a vertical acceleration record, it can be simply expressed as a sum of decaying cosinusoids [e.g., Aki and Richards 1980, Chao and Gilbert 1980, Master and Gilbert 1983, Master and Widmer-Schnidrig 1995]:

$$a(t) = \sum_{j}^{M} A_j \cos(\omega_j t + \phi_j) e^{-\alpha_j t}, \tag{1}$$

where A_j is the amplitude, α_j the attenuation, ω_j the frequency and ϕ_j the phase of the jth mode. And the quality factor Q of the jth mode can be estimated through ω_j and α_j, by the following equation

$$Q_j = \frac{\omega_j}{2\alpha_j} \tag{2}$$

According to Equation (2), one needs only to know the complex frequency of a mode, and then the corresponding Q can be estimated. There are numerous complex frequency estimation methods. Smith [1972] reviewed the early observations of α_j, most of which were obtained by the time lapse method. Chao and Gilbert [1980] proposed a method, referred to as the autoregressive (AR) method, to estimate the complex frequencies. Masters and Gilbert [1983] proposed a nonlinear least-squares fitting method, named as least-squares (LS) algorithm. Roult and Clévédé [2000] proposed an improved method, which is based on the 'time lapse' method, to estimate the attenuation α_j. Rosat et al. [2008] proposed a non-linear damped harmonic analysis (NLDHA) method, which can be also used to estimate the complex frequencies of a normal mode. In addition, the complex frequencies can be also estimated by fitting a Lorentzian function [e.g., Smylie 1992, Abd El-Gelil et al. 2010]. Here we should note that we just want to give a short review about those presented methods, rather than to explain their strengths and weaknesses. In this study, due to the fact that the validity of the AR method has been verified by previous studies [Chao 1983, Masters and Gilbert 1983], we use this method to estimate the complex frequencies of those modes. Because the details of the estimation process have been introduced in Chao and Gilbert [1980], here we only provide a brief introduction of the basic idea.

For a discrete time series (with N data points), set $\sigma_j = \omega_j + i\alpha_j$ and $\mathbf{A}_j = A_j e^{i\phi_j}$, then Equation (1) can be rewritten as,

$$a(n) = \sum_{j=1}^{M} \left[A_j \exp(in\sigma_j) + A_j^* \exp(in\sigma_j^*)\right], \; n = 1,2,\ldots,N \tag{3}$$

where ' * ' denotes complex conjugate, M denotes the number of the complex exponential functions. Then $a(n)$ can be expressed as the following linear equation,

$$a(n) = \sum_{i=1}^{2M} S_i a(n-1), \;\; n = 2M+1,\ldots,N \tag{4}$$

where S_i is a real constant coefficient ($i = 1,2,\ldots,2M$). According to the Prony method [e.g., Chao and Gilbert 1980, Chao 1990a], the relationship between $\{\sigma_j\}$ and $\{S_i\}$ can be constructed through the following polynomial equation

$$\begin{aligned} &Z^{2M} - S_1 Z^{2M-1} - S_2 Z^{2M-2} - \ldots - S_{2M} = \\ &= \prod_{j=1}^{M} \left[Z - \exp(i\sigma_j)\right]\left[Z - \exp(i\sigma_j^*)\right] = \\ &= \prod_{j=1}^{M} \left[Z^2 + p_j Z + q_j\right] \end{aligned} \tag{5}$$

where $\alpha_j = -0.5\ln q_i$ and $\omega_j = \cos^{-1}\left(-p_j/(2\sqrt{q_i})\right)$. Therefore, if $\{S_i\}$ are obtained, $\{\sigma_j\}$ can be determined by Equation (3). However, for a time series after an earthquake, M is usually unknown; that means one cannot solve Equation (4) for $\{S_i\}$ in the time domain. Fortunately, different modes could be separated into individual peaks in the frequency domain (for most of the normal modes). The technique is stated as follows. The Fourier transform (FT) of Equation (4) can be expressed as

$$X_0(\omega_k) = \sum_{i=1}^{2M} X_1(\omega_k) S_i \, , \quad k = 1,2,\ldots,K \tag{6}$$

where $\{X_i(\omega_k), i = 1,2,\ldots,2M\}$ corresponds to the Fourier transform of $\{a(n-i), \mathrm{n} = 2M+1,\ldots,N\}$. It can be also written as the matrix form

$$\begin{bmatrix} X_1(\omega_1) & X_2(\omega_1) & & X_{2M}(\omega_1) \\ X_1(\omega_2) & X_2(\omega_2) & & X_{2M}(\omega_2) \\ \vdots & \vdots & \ddots & \vdots \\ X_1(\omega_K) & X_2(\omega_K) & & X_{2M}(\omega_K) \end{bmatrix} \begin{bmatrix} S_1 \\ S_2 \\ \vdots \\ S_{2M} \end{bmatrix} = \begin{bmatrix} X_0(\omega_1) \\ X_0(\omega_2) \\ \vdots \\ X_0(\omega_K) \end{bmatrix} \tag{7}$$

It should be noted that a Hanning taper should be multiplied by each new time sequence prior to FT to weaken the spectral leakage. In addition, M becomes the number of the cosinusoids residing in the target frequency band. It is 1 for a single peak, and it is a small number for a group of interfering peaks with close frequencies and for some strongly coupled normal modes or splitting of a multiplet [Chao and Gilbert 1980, Chao 1990a, 1990b]. Here we only take M=1 as an example, and then, there are only two AR coefficients S_1 and S_2. However, considering that $X_i(\omega_k)$ has a real part and an imaginary part, if K=1, Equation (6) can be rewritten as the matrix form

$$\begin{bmatrix} \mathrm{Re}\left[X_2(\omega_1)\right] & \mathrm{Re}\left[X_1(\omega_1)\right] \\ \mathrm{Im}\left[X_2(\omega_1)\right] & \mathrm{Im}\left[X_1(\omega_1)\right] \end{bmatrix} \cdot \begin{bmatrix} S_1 \\ S_2 \end{bmatrix} = \begin{bmatrix} \mathrm{Re}\left[X_0(\omega_1)\right] \\ \mathrm{Im}\left[X_0(\omega_1)\right] \end{bmatrix} \tag{8}$$

Hence, taking K=M is enough to solve out $\{S_i\}$ from Equation (7). And if $K > M$, a simple way to solve Equation (7) is the linear least-squares estimate. After $\{S_i\}$ are found, $\{\sigma_j\}$ can be determined by using some numerical methods. The estimation of the complex amplitudes $\{\mathbf{A}_j\}$ is another problem of linear least-squares estimate, which is referred to Chao and Gilbert [1980] for details.

The above process is known as the AR method. And from Equation (7), one can see that this method has the capability to process multiple records simultaneously to enhance the signal to noise ratio (SNR), namely, one can stack the matrix from different records obtained from different stations. Furthermore, the records even can be obtained after different earthquakes. It is noted that the AR method is very powerful in estimating the parameters (complex frequency and amplitude) of the singlets of a multiplet simultaneously [Chao 1990a].

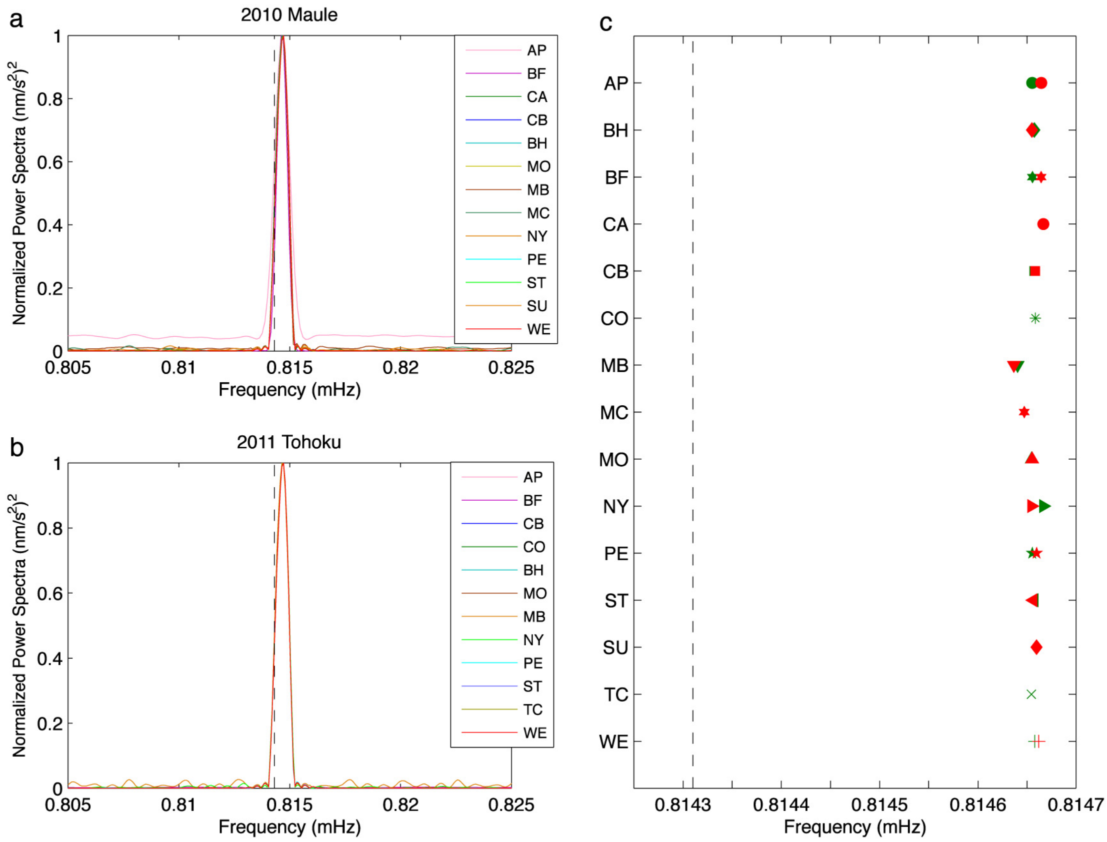

Figure 2. The power spectra of ${}_0S_0$. (a) The results of 13 residual gravity time series after the 2010 Maule event; (b) the results of 12 residual gravity time series after the 2011 Tohoku; (c) the estimated frequencies from different series, the red symbols (e.g., circle point, squares, etc.) indicate the results obtained from the 2010 event, and the green ones indicate the results obtained from the 2011 event (hereafter the same). The corresponding theoretical frequency based on PREM is denoted by vertical dashed lines.

${}_0S_0$	**Frequency (mHz)**	Q
PREM	0.81431	5327
Sailor and Dziewonski [1978]	0.814564	4229
Buland et al. [1979]	0.8146346±2.4e-5	4100±1066
Riedesel et al. [1980]	0.814664±3.3e-6	5700±285
Chao and Gilbert [1980]	0.814695±2.0e-5	5280±25
Roult et al. [2006]	0.814661±5.0e-6	5489.1±19.0
Rosat et al.[2007]	0.8146566±1.6e-6	5506±19
Xu et al. [2008]	0.8146565±1.2e-6	5400.94±22.4
Abd El-Gelil et al. [2010]	0.814666±0.7e-6	5551.0 ± 9.1
Zábranová et al. [2012]	--	5500±140
This paper (Average value)	0.8146568±6.5e-7	5566.6±18.8

Table 1. Observed weighted average values of the frequencies and Qs of ${}_0S_0$, and the model predictions and observations of previous studies.

Due to the fact that the SNRs of different records from the same event and those of the records from the same station after the two events are different, and some singlets of a mode may appear in a record but not appear in some other records, we use AR method to estimate the singlets of one target mode from each separated record, and take the weighted average of all of the estimates as the final estimation.

As for the estimated error, we prefer to use the bootstrap method [see e.g., Efron and Tibshirani 1986] as suggested by Häfner and Widmer-Schnidrig [2013], where the details were presented. After the estimated errors σ_j of a singlet frequency from different chosen SG records are obtained, the following step is carried out to get a final estimation.

For a given singlet after the two earthquakes, $1/\sigma^2$ is used as a weight to obtain the finally estimated frequency. The weight for the i-th observed singlet frequency from a chosen SG series is given by

$$P_i = (1/\sigma_i^2)\Big/\sum_i^N 1/\sigma_i^2 \tag{9}$$

where N is the number of all of the chosen series after the two events, σ_i is the estimated error of the estimated frequency, and the denominator $\sum_i^N 1/\sigma_i^2$ is applied to make $\sum_i^N 1/\sigma_i^2 = 1$. For each singlet, we use the following formula [Taylor 1997] to obtain a final estimate of the corresponding frequency based on the records after both earthquakes:

$$f_f = \sum_{i=1}^{n} P_i \cdot f_i\,,\ \ e(f_f) = \sqrt{\sum_{i=1}^{n} (P_i \cdot e(f_i))^2} \tag{10}$$

where f_f is the finally estimated frequency value for a given singlet, $e(f_f)$ its error, P_i the weight given by Equation (9), f_i and $e(f_i)$ are the estimates of the corresponding frequency value and its corresponding error bar for each chosen SG series.

3. The observations of different modes based on SG records

In this study, as mentioned in Section 1, concerning observing different modes, we use the records from different stations, due to the fact that different stations are differently sentsitive to different modes.

3.1. The frequencies and Qs of the modes ${}_0S_0$, ${}_0S_2$, ${}_0S_3$

Concerning the mode ${}_0S_0$, we use the SG residual time series from the first group of 13 stations (see Section 1) after the 2010 Maule event and the second group of 12 stations (except for the MC station) after the 2011 Tohoku event, with a length of 750h. The power spectra are shown in Figure 2, and for the same event, owing to the fact that the amplitudes of different records are not the same, the normalized power spectra are formulated for comparison (hereafter the same). The final estimation provided by this study is the weighted average of the 23 results estimated separately from each of all of the time series (hereafter, the same rule holds throughout this paper except for a special statement), which is provided in Table 1. For a comparative purpose, the results of previous studies and the theoretical predictions are also listed in Table 1. From Figure 2a,b, we find that the observed peaks of ${}_0S_0$ from different records are almost overlapped, and from Figure 2c and Table 1, there is a large deviation between our frequency estimate and the corresponding theoretical prediction of PREM [Dziewonski and Anderson 1981], but our result is very close to those given by previous studies. The Q value is about 5500, which is in consistent with PREM prediction and previous results.

Concerning the mode ${}_0S_2$, we use nine residual gravity time series after the 2010 Maule event and 11 residual gravity time series after the 2011 Tohoku event (see Figure 3), with a length of 300h. The other records are not used because the SNRs of them are not high enough (hereafter the same reason for using different records after the two events). The corresponding power spectra are plotted in Figure 3. Comparing with the results excited by the 2004 Sumatra earthquake [e.g., Rosat et al. 2005, Roult et al. 2010], the singlets $m=0$ excited by the 2010 Maule event and 2011 Tohoku event are both quite weak, and there is no detectable peak for the singlet $m=0$ in the SG time series after the 2010 event, whereas it can be only weakly observed in three SG time series (from BF, MB, and ST stations) after the 2011 event. In addition, excited by the 2004 Sumatra event, the amplitudes of $m=0$ and $m=\pm2$ are larger than the amplitudes of $m=\pm1$; whereas excited by the 2010 and 2011 event, the amplitudes of $m=\pm1$ are much larger than the amplitudes of $m=0$ and $m=\pm2$. This phenomenon is related to the focal mechanism and geographical locations of different earthquakes.

The observed weighted average values of the frequencies and Qs of ${}_0S_2$, and the corresponding theoretical predictions of PREM [Millot-Langet et al. 2003, Rosat et al. 2008] and some previous estimates are listed in Table 2. The estimated results of the frequencies and Qs are very close to the results of the previous studies as well as the PREM predictions.

We use eight residual gravity time series after the 2010 event and 12 residual gravity time series after the 2011 event to detect the mode ${}_0S_3$ (see Figure 4). The length of each sequence is 350 h. The power spectra and the estimated frequencies are shown in Figure 4. Comparing with Rosat et al. [2005]'s result (see Figure 2 therein) observed at the ST station after the 2004 Sumatra event, the mode ${}_0S_3$ observed at the ST station after three different earthquakes are quite different. The amplitudes of $m=\pm2$ excited by the 2010 and 2011 event are relatively larger. The observed average values of the frequencies and Qs of ${}_0S_3$ are listed in Table 3.

3.2. The frequencies and Qs of the modes ${}_2S_1$ and ${}_3S_1$

We use five residual gravity time series after the 2010 event and another five residual gravity time series after the 2011 event to detect the mode ${}_2S_1$ (see Figure 5), with a length of 168h. From Figure 5, we find that the singlet $m=0$ is clearly observed based on the SG records with high SNRs after the two earthquakes, whereas there are no records by which this singlet is observed

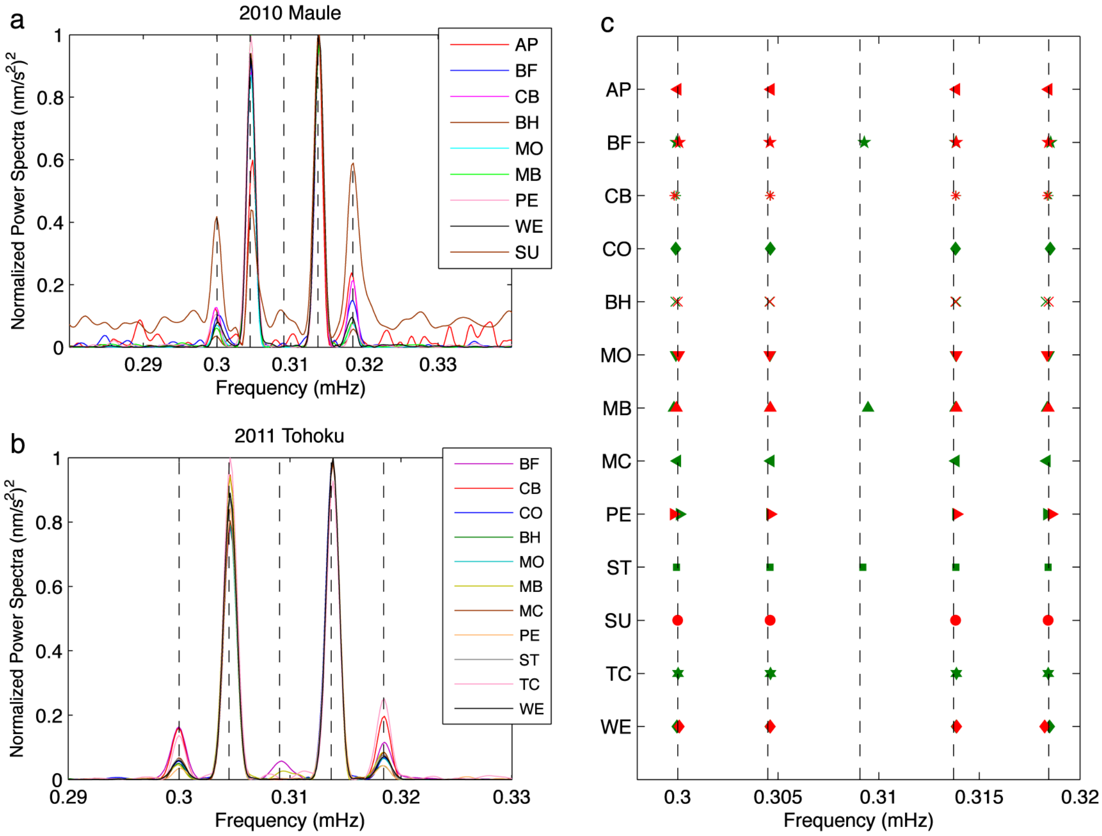

Figure 3. The power spectra of $_0S_2$ based on the residual gravity time series after the 2010 and 2011 events. (a) The results of 9 residual gravity time series after the 2010 Maule event; (b) the results of 11 residual gravity time series after the 2011 Tohoku; (c) the estimated frequencies from different series. The PREM predictions (from Rosat et al. [2008]) are denoted by vertical dashed lines.

$_0S_2$		$m=-2$	$m=-1$	$m=0$	$m=+1$	$m=+2$
PREM*	f	0.30000117	0.30449303	0.30906353	0.31371556	0.31845238
	Q	494.6	501.8	509.3	517.0	525.0
Buland et al. [1979]	f	0.30001	0.30480	0.30949	0.31400	0.31850
Rosat et al. [2005]	f	0.29997±6.3e-6	0.30458±4.7e-6	0.30924±6.0e-6	0.31381±1.1e-5	0.31843±4.6e-6
Roult et al. [2006]	f	0.299779±7.4e-5	0.304624±2.9e-5	0.309397±1.57e-4	0.313892±6.9e-5	0.318465±8.9e-5
	Q	490.6±14.0	562.9±4.0	395.6±11.3	495.3±4.0	480.2±14.9
Rosat et al. [2008] §	f	0.299951±1.5e-6	0.304599±1.6e-6	0.3092607±2.5e-7	0.3138446±2.6e-7	0.3184385±2.8e-7
	Q	449.3±0.1	481.5±0.1	506.7±0.4	457.7±0.3	518.7±0.4
Abd El-Gelil et al. [2010]	f	0.300001±1.2e-6	0.304533±1.1e-6	0.309296±1.1e-6	0.313882±0.5e-6	0.318402±1.0e-6
	Q	509.9±3.9	677.9±11.5	512.3±3.9	592.7±8.1	520.3±3.1
Roult et al. [2010]	f	0.29998±3.313e-4	0.30447±4.985e-4	0.30922±3.560e-4	0.31374±4.480e-4	0.31835±3.548e-4
Deuss et al. [2011]	f	0.29993	0.30463	0.30928	0.31386	0.31840
Rosat et al. [2012] #	f	0.29996±2.2e-5	0.30458±5.1e-5	0.30925±3.3e-5	0.31383±4.6e-5	0.31844±2.1e-5
Häfner and Widmer-Schnidrig [2013]	f	0.299948±9.0e-6	0.304612±6.0e-6	0.309269±1.6e-5	0.313840±5.0e-6	0.318429±9.0e-6
This paper (average value)	f	0.299958±8.1e-6	0.304588±4.6e-6	0.309263±1.1e-5	0.313835±1.4e-6	0.318422±7.4e-6
	Q	509.4±12.1	484.7±9.3	394.4±14.3	520.2±8.1	532.7±10.1

Table 2. The observed weighted average values of the frequencies and Qs of $_0S_2$, compared with the previous estimates and the PREM predictions. (*): from Millot-Langet et al. [2003], Rosat et al. [2008]. (§): the results using the NLDHA method based on one SG record (ST) after the 2004 Sumatra earthquake. (#): correction to Rosat et al. [2005].

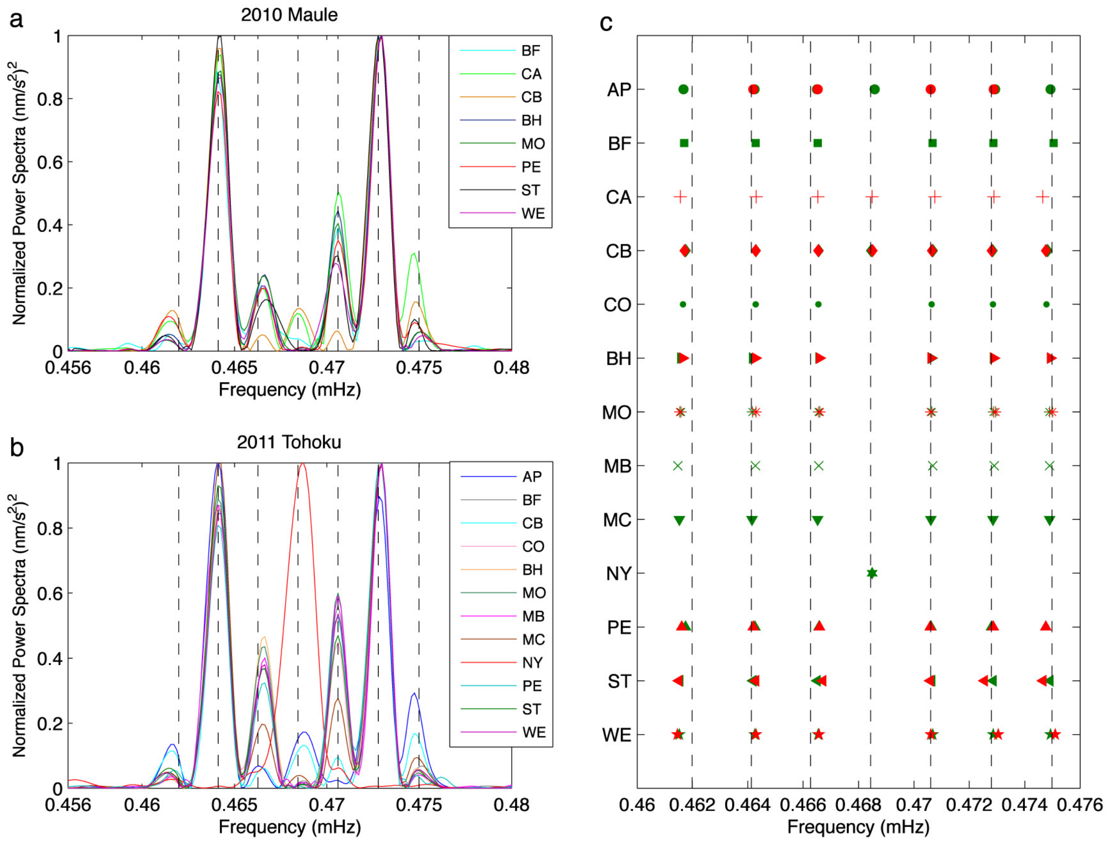

Figure 4. The power spectra of ${}_0S_3$ based on the residual gravity time series after the 2010 and 2011 events. (a) The results of 8 residual gravity time series after the 2010 Maule event; (b) the results of 12 residual gravity time series after the 2011 Tohoku; (c) the estimated frequencies from different series. The PREM predictions (from Rosat et al. [2008]) are denoted by vertical dashed lines.

${}_0S_3$		m=−3	m=−2	m=−1	m=0	m=+1	m=+2	m=+3
PREM*	*f*	0.4618	0.4641	0.4664	0.4686	0.4707	0.4728	0.4748
	Q	411.7	413.6	415.5	417.4	419.3	421.3	423.3
Buland et al. [1979]	*f*	0.46167	0.46408	0.46617	0.46883	0.47091	0.47317	0.47450
Rosat et al. [2005]	*f*	0.46167 ±3.0e-5	0.46424 ±2.0e-5	0.46639 ±1.8e-5	-	0.47084 ±1.1e-5	0.47266 ±4.8e-5	0.47474 ±2.1e-5
Roult et al. [2006]	*f*	0.461646 ±8.7e-5	0.464329 ±7.1e-5	0.466236 ±8.3e-5	0.468560 ±4.2e-5	0.470877 ±5.2e-5	0.472659 ±1.33e-4	0.474269 ±4.68e-4
	Q	450.5±63.3	442.5±46.3	456.6±93.0	434.2±19.3	339.9±68.9	493.9±56.3	382.6±39.2
Rosat et al. [2008] §	*f*	0.4615728 ±4.9e-6	0.4642270 ±4.9e-6	0.4664168 ±4.6e-7	-	0.4707937 ±3.8 e-6	0.4727150 ±6.9e-6	0.4747854 ±1.1 e-6
	Q	380.3±0.04	412.7±0.1	447.5±0.5	-	446.1±0.1	477.2±0.2	328.2±0.3
Abd El-Gelil et al. [2010]	*f*	0.461662 ±0.4e-6	0.464377 ±0.5e-6	0.466121 ±0.2e-6	0.468456 ±0.2e-6	0.470920 ±0.3e-6	0.472505 ±0.7e-6	0.474535 ±2.1e-6
	Q	393.2±8.2	474.5±24.7	466.6±25.6	468.5±18.4	501.5±32.4	573.4±41.5	605.3±49.4
Roult et al. [2010]	*f*	0.46169 ±3.515e-4	0.46417 ±3.480e-4	0.46640 ±4.036e-4	0.46860 ±4.220e-4	0.47076 ±1.760e-4	0.47275 ±4.059e-	0.47470 ±1.786e-4
Rosat et al. [2012] #	*f*	0.46167 ±5.4e-5	0.46424 ±7.8e-5	0.46639 ±3.6e-5	-	0.47084 ±3.0e-5	0.47266 ±7.8e-5	0.47474 ±6.8e-5
This paper (average value)	*f*	0.461623 ±4.9e-6	0.464219 ±1.8e-6	0.466535 ±2.6e-6	0.468549 ±5.2e-6	0.470657 ±2.4e-6	0.472843 ±1.7e-6	0.474831 ±3.5e-6
	Q	351.5±19.1	418.5±9.2	348.4±15.8	424.4±22.5	356.9±14.5	397.7±10.0	417.2±16.3

Table 3. The observed and predicted values of the frequencies (mHz) and Qs of ${}_0S_3$. (*): from Millot-Langet et al. [2003], Rosat et al. [2008]. (§): the results using the NLDHA method based on one SG record (ST) after the 2004 Sumatra earthquake. (#): correction to Rosat et al. [2005].

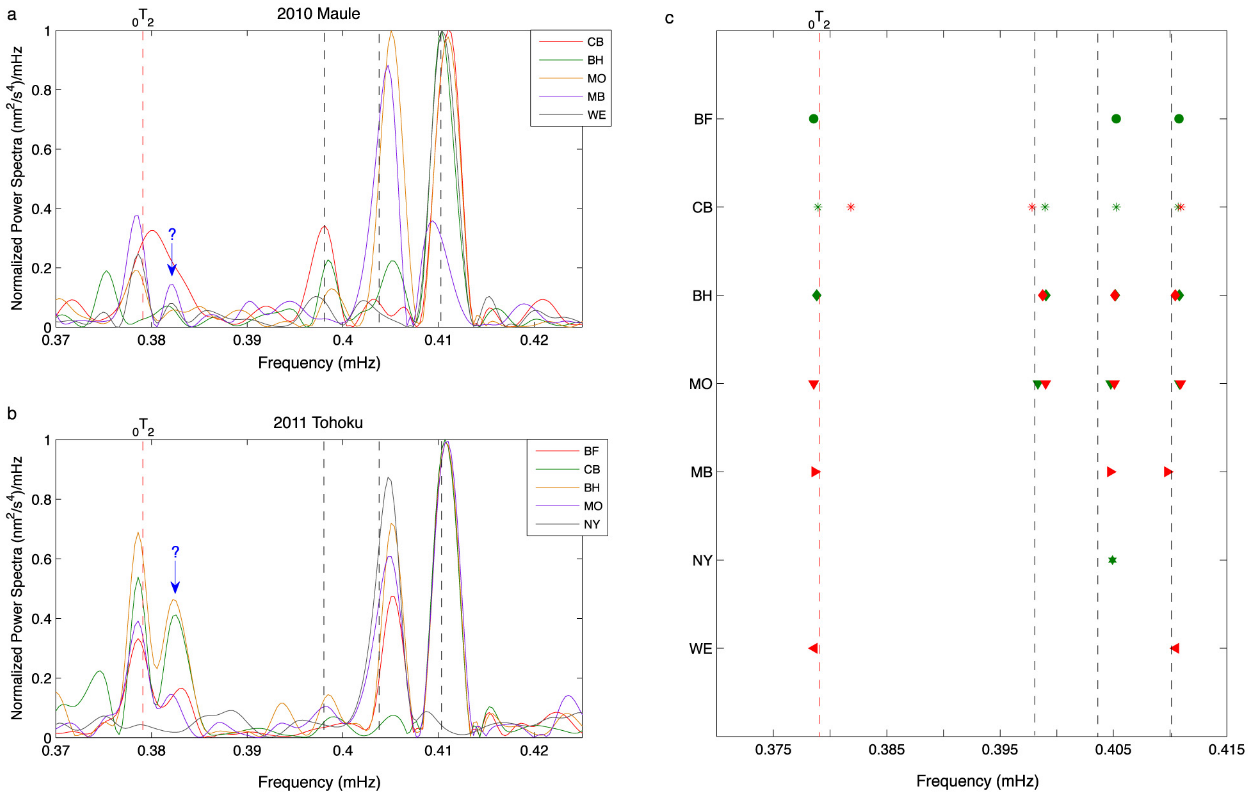

Figure 5. The power spectra of $_2S_1$ based on the residual gravity time series after the 2010 and 2011 events. (a) The results of 5 residual gravity time series after the 2010 Maule event; (b) the results of 5 residual gravity time series after the 2011 Tohoku; (c) the estimated frequencies from different series. The PREM predictions are denoted by vertical dashed lines (for $_2S_1$, the three values are from Roult et al. [2006] denoted by black vertical dashed lines; for $_0T_2$, the value is from Dziewonski and Anderson [1981], denoted by red vertical dashed line).

$_2S_1$	PREM*		Rosat et al. [2003]	Rosat et al. [2005]	Roult et al. [2006]		Roult et al. [2010]	Deuss et al. [2011]	This paper (average value)	
	f(mHz)	Q	f(mHz)	f(mHz)	f(mHz)	Q	f(mHz)	f(mHz)	f(mHz)	Q
$m=-1$	0.39803582	391.1	0.3986 ±1.9e-4	0.39821 ±6.0e-5	0.39510	368.8	0.39779 ±2.543e-3	0.39792	0.398662 ±8.5e-6	365.9±20.3
$m=0$	0.40368712	396.6	0.4049 ±2.1e-4	-	0.40645	428.2	0.40394 ±1.352e-3	0.40518	0.405014 ±2.7e-6	448.3±15.7
$m=+1$	0.41022196	403.1	0.4111 ±1.8e-4	0.41080 ±4.2e-5	0.41184	322.1	0.41063 ±1.012e-3	0.41045	0.410768 ±1.2e-6	385.6±11.8

Table 4. The observed and predicted values of frequencies and Qs of $_2S_1$. (*): from Millot-Langet et al. [2003], Roult et al. [2006].

after the 2004 Sumatra event [see Rosat et al. 2005]. In addition, the toroidal mode $_0T_2$, which is coupled with the mode $_2S_1$, is also observed in the spectra, and there is a very clear peak around 0.3826 mHz, which may correspond to the singlet m=2 of $_0T_2$ (see Roult et al. [2010]). From Figure 5c and Table 4, there is a large deviation between our frequency estimates with the results of Roult et al. [2006], but our results are very close to the results of Rosat et al. [2003, 2005] and Deuss et al. [2011]. Moreover, comparing with the PREM predictions [Millot-Langet et al. 2003, Roult et al. 2006], our results perform a total shift toward a higher frequency. Concerning the observed Q-values of $_2S_1$, different authors give different results (see Table 4), and our results show that the Q-values are between 360 and 450. Here we note that the estimated frequency and Q value of $_0T_2$ are listed in Table 7.

As for the mode $_3S_1$, in order to weaken the interference of $_1S_3$, we use three SG records starting 50h after the 2010 event and seven SG records starting 50h after the 2011 event (see Figure 6), the data length of each record is taken as 680h. From Figure 6, there are no observable peaks for $_2S_2$ and $_1S_3$ (blue dotted curves), but the triplet (especially the singlet m=0) of $_3S_1$ is clearly

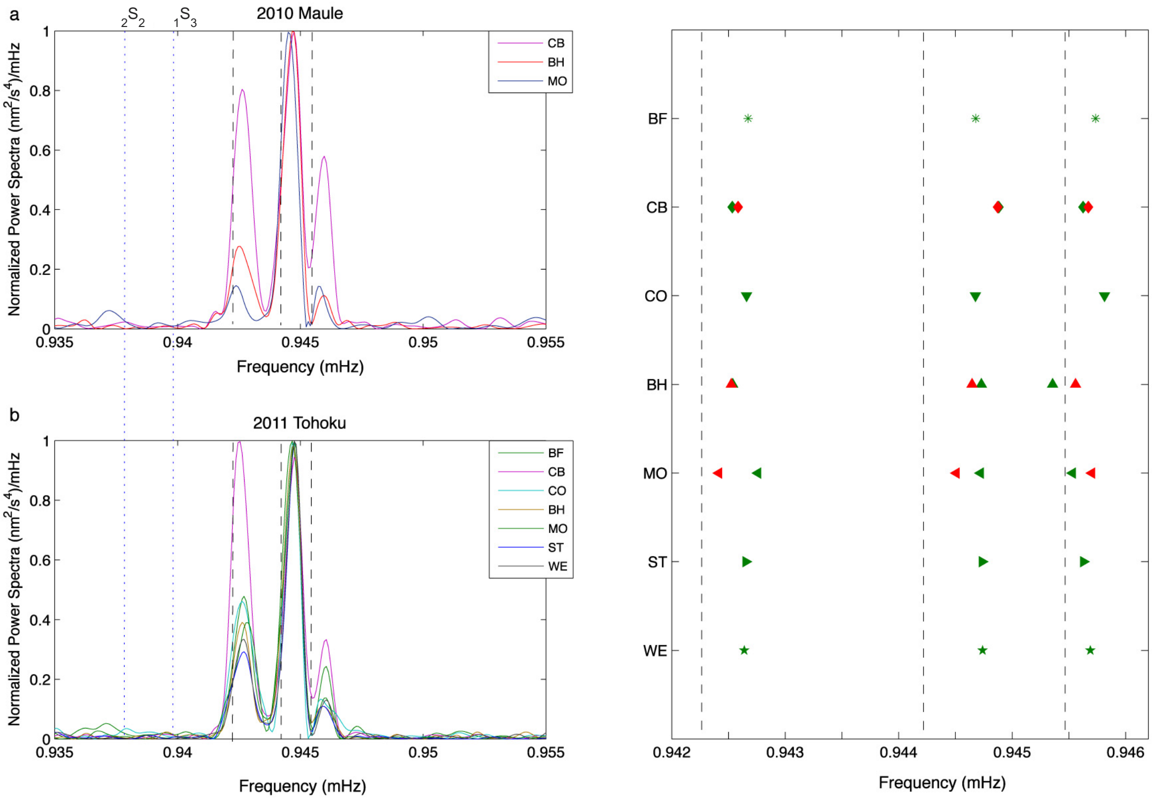

Figure 6. The power spectra of $_3S_1$ based on the SG sequences after the 2010 and 2011 events. (a) The results of 3 residual gravity time series after the 2010 Maule event; (b) the results of 7 residual gravity time series after the 2011 Tohoku; (c) the estimated frequencies from different series. The PREM predictions (from Roult et al. [2010]) are denoted by vertical dashed lines.

$_3S_1$	PREM*	Chao and Gilbert [1980]		Roult et al. [2010]	Shen and Wu [2012]	This paper (average value)	
	f(mHz)	f(mHz)	Q	f(mHz)	f(mHz)	f(mHz)	Q
m=−1	0.942267	0.94270±5.5e-5	884±0.11	0.94256±1.241e-4	0.942598 ±4.20e-4	0.942426±2.5e-6	943.8±12.5
m=0	0.944217	0.94535±9.0e-5	1450±0.2	0.94419±3.444e-4	0.944113 ±2.65e-4	0.944713±1.7e-6	773.6±10.1
m=+1	0.945472	0.94563±4.0e-5	890±0.08	0.94579±1.493e-4	0.945864 ±2.13e-4	0.945612±4.6e-6	629.5±18.4

Table 5. The predictions and observations of frequencies and Qs of $_3S_1$. (*): from Roult et al. [2010].

observed in the direct power spectra of the series.

Some studies [e.g., Giardini et al. 1988, Widmer-Schnidrig et al. 1992a] considered that the $_3S_1$ was anomalously split. For example, Widmer-Schnidrig et al. [1992a] declared that $_3S_1$ was anomalously split based upon the observations of the m=0 singlet using only the record from the Amundsen-Scott South Pole station, but the SNR of their observations is not high, and the length of the data is only 100h long (far less than the 1.1Q-cycle), which may not provide a sufficient frequency resolution. Moreover, according to the results of Roult et al. [2010], there are only the singlets m=±1 which are excited to the detectable level by the 2004 Sumatra event. Our results show that all of the three singlets are excited to the detectable level by the 2010 and 2011 events, and the amplitude of m=0 is even larger than that of m=±1 (Figure 6). In addition, our results show a systematic shift from the PREM predictions toward a higher frequency (see Figure 6c and Table 5). The observed weighted average values of Qs of $_3S_1$ are also listed in Table 5. If we accept the statement that a multiplet is anomalously split if the splitting width ratio R (ratio of observed splitting width to the predicted splitting width) is larger than 1.5 [Widmer-Schnidrig et al. 1992a], then according to Table 5, our results (R=0.99) suggest that $_3S_1$ is a normally split mode (consistent with the result of Roult et al. [2010]).

3.3. The frequencies and Qs of the modes $_0S_4$ and $_1S_2$

In order to identify all of the singlets of $_0S_4$, a very long record should be used. However, the SNRs of the modes will gradually decrease with the increase

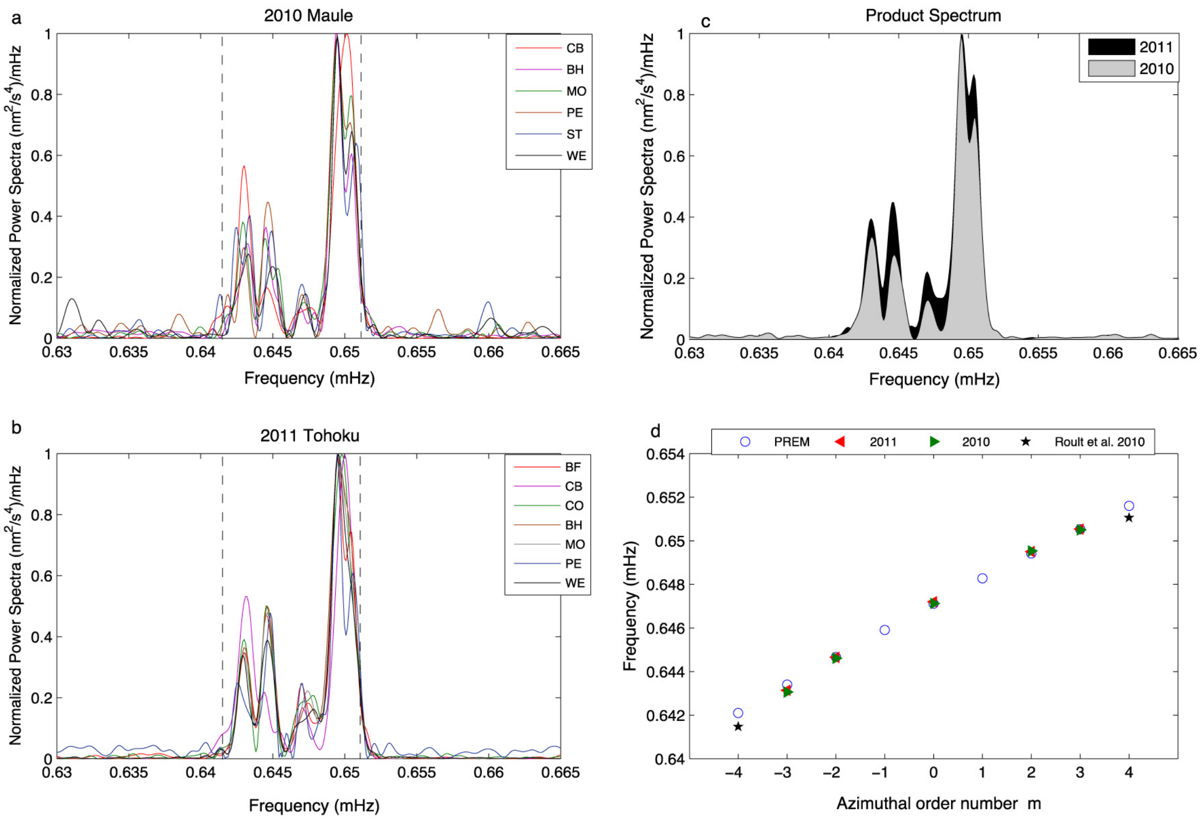

Figure 7. The spectra of ${}_0S_4$. (a) The results after the 2010 Maule event; (b) the results after the 2011 Tohoku; (c) the product spectra of the residual gravity time series after each of the two events; (d) the distributions of the estimated frequencies and the corresponding PREM predictions. The dashed vertical lines indicate the observed frequencies of the singlets $m=\pm4$ observed by Roult et al. [2010].

		f(mHz)	Q			f(mHz)	Q
${}_0S_4$	$m=-3$	0.631015±2.2e-6	292.7±14.1	${}_1S_2$	$m=-2$	0.673533±3.2e-6	325.7±9.5
	$m=-2$	0.644624±2.4e-6	354.3±12.5		$m=-1$	0.677671±1.2e-6	312.3±5.8
	$m=0$	0.64715±5.5e-6	325.1±15.7		$m=0$	0.680915±7.4e-6	269.9±16.7
	$m=+2$	0.649545±4.5e-7	349.6±6.8		$m=+1$	0.683541±1.7e-6	270.4±6.4
	$m=+3$	0.650534±5.9e-7	462.8±7.2		$m=+2$	0.685372±3.4e-6	279.3±10.3

Table 6. The observed weighted average values of frequencies and Qs of ${}_0S_4$ and ${}_1S_2$ in this study.

of the length of data. Hence, there must be a trade-off between the chosen data length and the SNR. In this paper, 13 residual gravity time series with a length of 550h are chosen to observe the ${}_0S_4$ modes (see Figure 7). The power spectra of the ${}_0S_4$ modes are shown in Figure 7a,b, and the product spectra of the series after each of the two events are shown in Figure 7c. The two dashed vertical lines (Figure 7a,b) indicate the observed frequencies of the singlets $m=\pm4$ given by Roult et al. [2010], and the PREM predictions [Roult et al. 2010] are shown in Figure 7d. There are only five singlets that can be found from the spectra, and according to Figure 7d, they are corresponding to the singlets $m=0$, $m=\pm2$, and $m=\pm3$. The estimated values of the corresponding frequencies and Qs are listed in Table 6. Here, the Qs of five singlets of ${}_0S_4$ were determined for the first time by observation.

Concerning the observation of the mode ${}_1S_2$, we use two SG records after the 2010 event and six SG records after the 2011 event (see Figure 8). Each of the time series has a length of 330h. The corresponding spectra are shown in Figure 8, and we find that there is no observable peak for the singlet $m=0$ after the 2010 event (Figure 8a), whereas all of the five singlets are observed after the 2011 Tohoku earthquake (Figure 8b). The PREM predictions are plotted in Figure 8 (dashed vertical lines), where the effects of rotation and ellipticity have been taken into account. The estimated weighted average values of the frequencies and Qs of

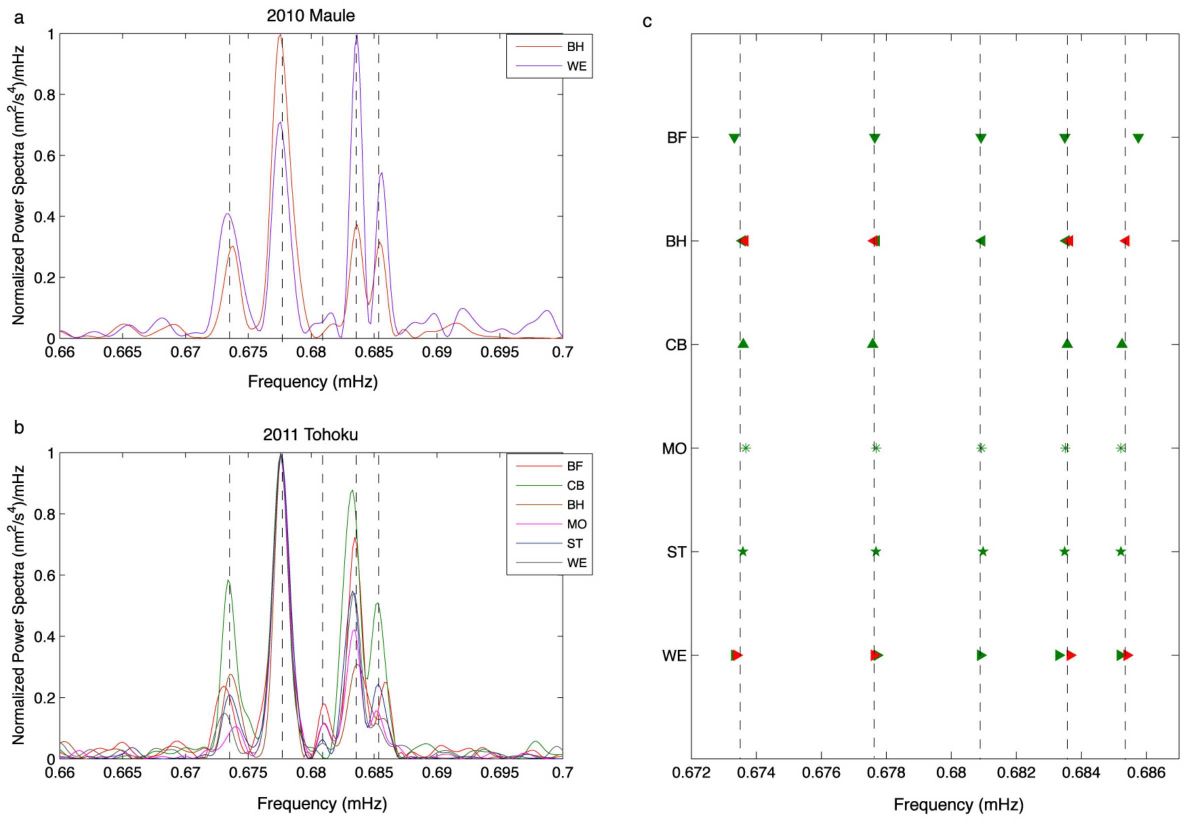

Figure 8. The power spectra of ${}_1S_2$ based on the residual gravity time series after the 2010 and 2011 events. (a) The results of two residual gravity time series after the 2010 Maule event; (b) the results of 6 residual gravity time series after the 2011 Tohoku; (c) the estimated frequencies from different series. The PREM predictions are denoted by vertical dashed lines.

		${}_0T_2$	${}_0T_3$	${}_0T_4$
PREM	*f* (mHz)	0.37917	0.58616	0.76566
	Q	250.4	240.0	228.2
Widmer-Schnidrig et al. [1992b]	*f* (mHz)	0.3766	0.58726	0.76673
	Q	--	222.2	265.3
Tromp and Zanzerkia [1995]	*f* (mHz)	--	--	0.76583
	Q	--	--	195
Hu et al. [2006]	*f* (mHz)	0.37823	0.58634	0.76586
Abd El-Gelil et al. [2010]	*f* (mHz)	0.37760	0.58690	0.76460
This paper (average value)	*f* (mHz)	0.379130±2.4e-6	0.586918±4.9e-7	0.765803±5.6e-7
	Q	271.6±14.2	232.9±8.4	242.4±9.5

Table 7. The observed weighted average values of frequencies and *Q*s of ${}_0T_2$, ${}_0T_3$, and ${}_0T_4$, compared to the PREM predictions and the results of some previous studies.

${}_1S_2$ are listed in Table 6. The PREM predictions of ${}_0S_4$ and ${}_1S_2$ are not tabulated in Table 6, which are referred to Roult et al. [2010]. It is noted that the *Q*s of the whole set of the singlets of ${}_1S_2$ are determined by observation for the first time in this study.

3.4. The frequencies and Qs of the toroidal modes ${}_0T_2$, ${}_0T_3$ and ${}_0T_4$

The power spectra of ${}_0T_2$ have been shown in Figure 5, and the estimated weighted average values of the frequencies and *Q*s are listed in Table 7.

For the purpose of observing the $_0T_3$ mode, we use five residual gravity time series after the 2010 event and four residual gravity time series after the 2011 event, each of them with a length of 70h. The power spectra are shown in Figure 9, where one can find that the results are larger than the theoretical predictions of PREM [Dziewonski and Anderson 1981].

Concerning the mode $_0T_4$, we use five residual gravity time series after the 2010 event (Figure 10a), each of the records with a length of 120h, and seven residual gravity time series after the 2011 event (Figure 10b), each of the series starting 5h after the event with a length of 80h. Here we choose the records with different lengths, because the SNRs of the records after the two events are significantly different. Due to different lengths (120h and 80h) of the records, the discrepancy of the frequency resolutions of the spectra of the two events is about 1.16μHz. From Figure 10c, we find that the discrepancy between the weighted average values obtained respectively from the records after the 2010 event and the 2011 event is only 0.48μHz, which is far less than 1.16μHz. This implies that both the results (based on respectively the records after the 2010 and 2011 events) are physically meaningful and should be used as parts of the estimates of the frequencies and *Q*s of the mode. Hence, the final results (see Table 7) of the frequencies and *Q*s are given by the weighted average of the 2010 and 2011 results.

The observed weighted average values of the frequencies and *Q*s of $_0T_2$, $_0T_3$, and $_0T_4$ are listed in Table 7. Comparing with the results of Widmer-Schnidrig et al. [1992b], Tromp and Zanzerkia [1995], Hu et al. [2006] and Abd El-Gelil et al. [2010], we provide additional estimates of the *Q*-values of the three modes, which are comparable with the corresponding PREM predictions.

4. Conclusions

After the 2010 Mw8.8 Maule earthquake and the 2011 Mw9.1 Tohoku earthquake, we used the SG records to determine the frequencies and *Q*s of the singlets of the modes below 1mHz based on the AR method proposed by Chao and Gilbert [1980]. The frequencies and *Q*s of all the singlets of the modes $_0S_2$, $_2S_1$, $_0S_3$, $_0S_0$, and $_3S_1$, and the frequencies of $_0S_4$, $_1S_2$, $_0T_2$, $_0T_3$, and $_0T_4$ were re-estimated. Moreover, the *Q*s of all of the five singlets of $_1S_2$, the *Q*s of the five singlets (m=0, m=±2, and m=±3) of $_0S_4$ and the *Q*s of $_0T_2$, $_0T_3$, and $_0T_4$ were first time or re-estimated by observation.

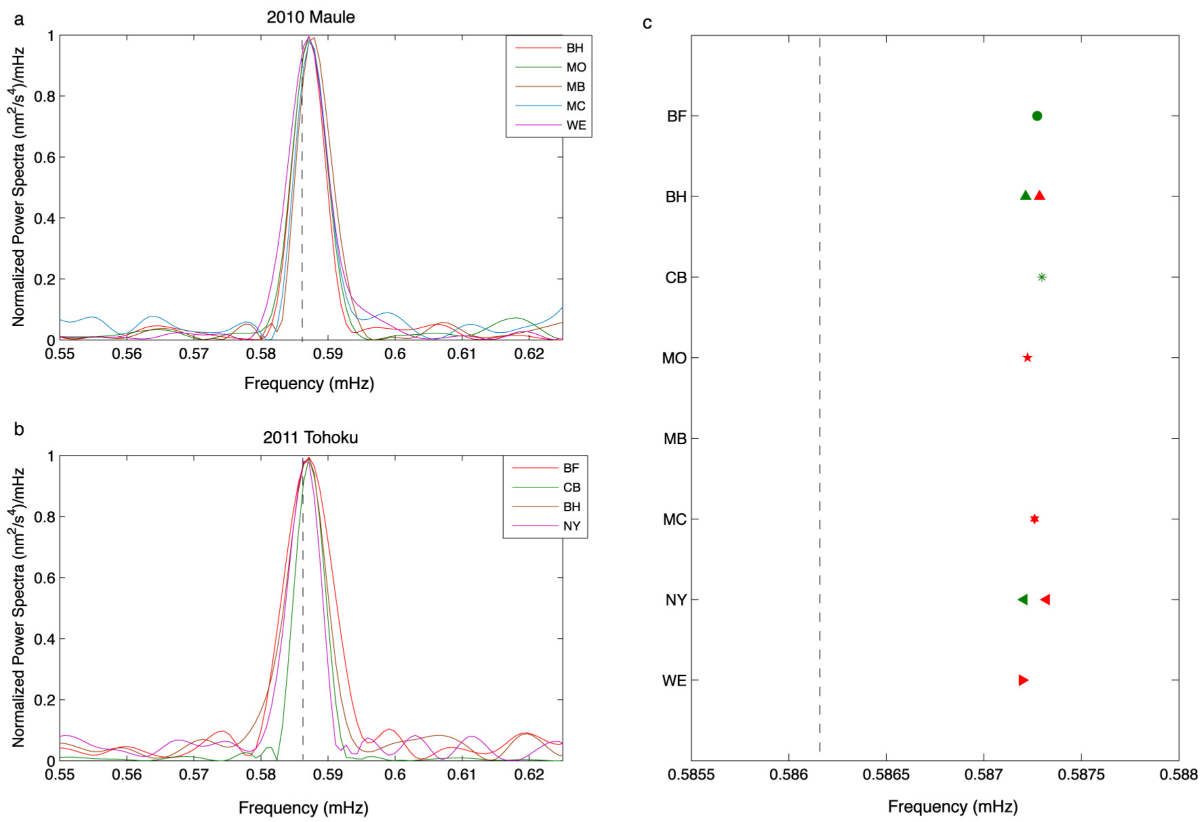

Figure 9. The power spectra of $_0T_3$ based on the residual gravity time series after the 2010 and 2011 events. (a) The results of 5 residual gravity time series after the 2010 Maule event; (b) the results of 4 residual gravity time series after the 2011 Tohoku; (c) the estimated frequencies from different series. The PREM prediction is denoted by the vertical dashed line. The red symbols indicate the results obtained from the 2010 event, and the green symbols indicate the results obtained from the 2011 event.

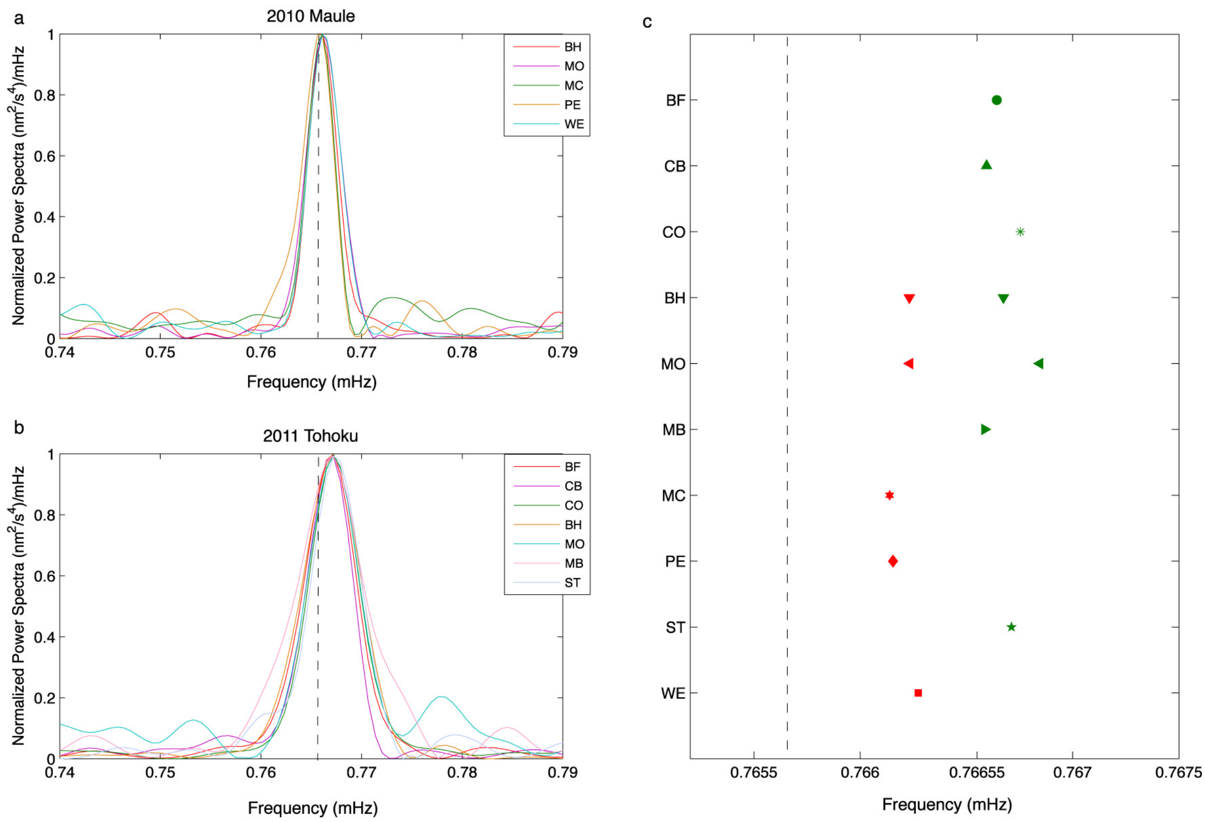

Figure 10. The power spectra of ${}_0T_4$. (a) The results of 5 residual gravity time series after the 2010 Maule event; (b) the results of 7 residual gravity time series after the 2011 Tohoku; (c) the estimated frequencies from different series. The residual gravity time series after the 2010 event have a length of 120h, and the series after the 2011 event have a length of 80h. The PREM prediction is denoted by the vertical dashed line.

In addition, the singlets m=0 of the modes ${}_2S_1$ and ${}_3S_1$ were clearly observed in the direct spectra of the residual gravity time series without using other special spectral analysis methods or special series of polar station records, especially for ${}_3S_1$. Due to the fact that, some studies considered that ${}_3S_1$ was anomalously split [e.g., Giardini et al. 1988, Widmer-Schnidrig et al. 1992a], while others [e.g., Ritzwoller et al. 1986, He and Tromp 1996, Roult et al. 2010] considered normal, a clear observation of the singlet m=0 may provide further evidence to judge whether ${}_3S_1$ is normally split. Taking into account the fact that the splitting width ratio R of ${}_3S_1$ obtained in this study is 0.99, we conclude that ${}_3S_1$ is normally split.

Comparing with previous studies, our results again clearly show that the amplitudes of the singlets of a given mode excited by different earthquakes (which have similar magnitude) are different (of course, it is a well-known statement). For instance, the singlet m=0 of ${}_2S_1$ cannot be observed using the SG records after the 2004 Mw9.0 Sumatra earthquake whereas it can be clearly observed from the SG residual sequences after the 2010 Mw8.8 Maule earthquake and the 2011 Mw9.1 Tohoku earthquake.

In summary, our estimations of the frequencies and Qs of the singlets of the modes below 1mHz provide further valuable information for constraining and refining the 3D density structure and attenuation models of the Earth.

Acknowledgements. The authors are grateful to the GGP station managers for the high-quality records; thank Professor B. F. Chao for his valuable comments during the preparation of the manuscript, and thank Editor Dr. Francesca Bianco and an anonymous Reviewer for their valuable comments and suggestions, which greatly improved the manuscript. This study is supported by NSFC (grant No. 41174011), National 973 Project China (grant No. 2013CB733305), NSFC (grant Nos. 41210006, 41128003, 41021061, 40974015), the Fundamental Research Funds for the Central Universities (grant No. 2012214020203), the Open Research Fund Program of the Key Laboratory of Geospace Environment and Geodesy, Ministry of Education, China (No. 12-02-04, 12-02-02), and the Open Fund of the State Key Laboratory of Geodesy and Earth's Dynamics, Institute of Geodesy and Geophysics, CAS (No. SKLGED2013-2-3-E).

References

Abd El-Gelil, M., S. Pagiatakis and A. El-Rabbany (2010). Normal mode detection and splitting after Sumatra–Andaman earthquake, J. Geodyn., 50, 49-56; doi:10.1016/j.jog.2010.02.003.

Aki, K., and P.G. Richards (1980). Quantitative seismology: theory and methods, W. H. Freeman, San Francisco.

Buland, R., J. Berger and F. Gilbert (1979). Observations from the IDA network of attenuation and splitting during a recent earthquake, Nature, 277, 358-362; doi:10.1038/277358a0.

Chao, B.F., and F. Gilbert (1980). Autoregressive estimation of complex eigenfrequencies in low frequency seismic spectra, Geophys. J. R. Astron. Soc., 63, 641-657; doi:10.1111/j.1365-246X.1980.tb02643.x.

Chao, B.F. (1983). Autoregressive Harmonic Analysis of the Earth's Polar Motion Using Homogeneous International Latitude Service Data, J. Geophys. Res., 88, B12, 10,299-10,307.

Chao, B.F. (1990a). Comment on "A New Method of Spectral Analysis and Its Application to the Earth's Free Oscillations: The "Sompi" Method" by S. Hori et al., J. Geophys. Res., 95 (B12), 19789-19790; doi:10.1029/JB095iB12p19789.

Chao, B.F. (1990b). On the use of maximum entropy-autoregressive spectrum in harmonic analysis of time series, Pageoph, 134 (2), 303-311; doi:10.1007/BF00877003.

Dahlen, F.A. (1982). The effect of data windows on the estimation of free oscillations parameters, Geophys. J. R. Astron. Soc., 69, 537-549; doi:10.1111/j.1365-246X.1982.tb04964.x.

Deuss, A., J. Ritsema and H. Heijst (2011). Splitting function measurements for Earth's longest period normal modes using recent large earthquakes, Geophys. Res. Lett., 38, L04303; doi:10.1029/2010GL046115.

Ding, H, and W.B. Shen (2013). Search for the Slichter modes based on a new method: optimal sequence estimation, J. Geophys. Res., 118 (8), 5018-5029.

Dziewonski, A.M., and D.L. Anderson (1981). Preliminary reference Earth model, Phys. Earth Planet. Int., 25, 297-356.

Efron, B., and R. Tibshirani (1986). Bootstrap methods for standard errors, confidence intervals, and other measures of statistical accuracy, Statist. Sci., 1, 54-77.

Giardini, D., X.D. Li and J.H. Woodhouse (1988). Splitting functions of long-period normal modes of the earth, J. Geophys. Res., 99, 13716-13742; doi:10.1029/JB093iB11p13716.

Häfner, R., and R. Widmer-Schnidrig (2013). Signature of 3D density structure in superconducting gravimeter spectra of the ${}_0S_2$ multiplet, Geophys. J. Int., 192, 285-294.

He, X., and J. Tromp (1996). Normal-mode constraints on the structure of the Earth, J. Geophys. Res., 110 (B9), 20053-20082; doi:10.1029/96JB01783.

Hu, X.G., L.T. Liu, J. Hinderer, H.T. Hsu and H.P. Sun (2006). Wavelet filter analysis of atmospheric pressure effects in the long-period seismic mode band, Phys. Earth Planet. Int., 154, 70-84; doi:10.1016/j.pepi.2005.09.003.

Masters, G., and F. Gilbert (1983). Attenuation in the earth at low frequencies, Phi. Trans. R. Soc. Lond., A308, 479-522; doi:10.1098/rsta.1983.0016.

Masters, G., R. Widmer (1995). Free oscillation: frequencies and attenuations, Global Earth Physics, A Handbook of Physical Constants, AGU Reference Shelf 1.

Millot-Langet, R., E. Clévédé and P. Lognonné (2003). Normal modes and long period seismograms in a 3D anelastic elliptical rotating Earth, Geophys. Res. Lett., 30, 1202-1206; doi:10.1029/2002GL016257.

Okal, E.A. (1978). A physical classification of the Earth's spheroidal modes, J. Geophys. Earth, 26, 75-103.

Resovsky, J.S., and M.H. Ritzwoller (1998). New and refined constrains on three-dimensional Earth structure from normal modes below 3 mHz, J. Geophys. Res., 103, 783-810; doi:10.1029/97JB02482.

Riedesel, M.A., D. Agnew, J. Berger and F. Gilbert (1980). Stacking for the frequencies and Qs of ${}_0S_0$ and ${}_1S_0$, Geophys. J. R. Astron. Soc., 62, 457-471; doi:10.1111/j.1365-246X.1980.tb04867.x.

Ritzwoller, M., G. Masters and F. Gilbert (1986). Observations of anomalous splitting and their interpretation in terms of aspherical structure, J. Geophys. Res., 91 (B10), 10203-10228; doi:10.1029/JB091iB10p10203

Rosat, S., J. Hinderer and L. River (2003). First observation of ${}_2S_1$ and study of the splitting of the football mode ${}_0S_2$ after the June 2001 Peru earthquake of magnitude 8.4, Geophys. Res. Lett., 30, 10-11; doi:10.1029/2003GL018304.

Rosat, S., T. Sato, Y. Imanishi, J. Hinderer, Y. Tamura, H. McQueen and M. Ohashi (2005). High- resolution analysis of the gravest seismic normal modes after the 2004 Mw = 9 Sumatra earthquake using superconducting gravimeter data, Geophys. Res. Lett., 32, L13304; doi:10.1029/2005GL023128.

Rosat, S., S. Watada and T. Sato (2007). Geographical variations of the ${}_0S_0$ normal mode amplitude: predictions and observations after the Sumatra-Andaman earthquake, Earth Planets Space, 59, 307-311.

Rosat, S., T. Fukushima, T. Sato and Y. Tamura (2008). Application of a non-linear damped harmonic analysis method to the normal modes of the Earth, J. Geodyn., 45, 63-71; doi:10.1016/j.jog.2007.06.001.

Rosat, S., and J. Hinderer (2011). Noise Levels of Superconducting Gravimeters: Updated Comparison and Time Stability, Bull. Seismol. Soc. Am., 101 (3), 1233-1241.

Rosat, S., T. Sato, Y. Imanishi, J. Hinderer, Y. Tamura, H. McQueen and M. Ohashi (2012). Correction to "High-resolution analysis of the gravest seismic normal modes after the 2004 Mw = 9 Sumatra earthquake using superconducting gravimeter data", Geophys. Res. Lett., 39, L22601; doi:10.1029/2012 GL054248.

Roult, G., and E. Clévédé (2000). New refinements in attenuation measurements from free-oscillation and surface-wave observations, Phys. Earth Planet. Inter., 121, 1-37; doi:10.1016/S0031-9201(00)00155-2.

Roult, G., S. Rosat, E. Clévédé, R. Millot-Langet and J. Hinderer (2006). New determinations of Q quality factors and eigenfrequencies for the whole set of singlets of the Earth's normal modes ${}_0S_0$, ${}_0S_2$, ${}_0S_3$ and ${}_2S_1$ using superconducting gravimeter data from the GGP network, J. Geodyn., 41, 345-357; doi:10.1016/j.jog.2005.08.020.

Roult, G., J.Roch and E. Clévédé (2010). Observation of split modes from the 26th December 2004 Sumatra-Andaman mega-event, Phys. Earth Planet. Int., 179, 45-59; doi:10.1016/j.pepi.2010.01.001.

Sailor, R.V., and A.M. Dziewonski (1978). Measurements and interpretation of normal mode attenuation, Geophys. J. R. Astron. Soc., 53, 559-581; doi:10. 1111/j.1365-246X.1978.tb03760.x.

Shen, W.B., and B. Wu (2012). A case study of detecting the triplet of ${}_3S_1$ using superconducting gravimeter records with an alternative data preprocessing technique, Annals of Geophysics, 55 (2), 293-300; doi:10. 4401/ag-4944.

Smith, S.W. (1972). The anelasticity of the mantle, Tectonophys, 13, 601-622; doi:10.1016/0040-1951(7 2)90040-6.

Smylie, D.E. (1992). The inner core translational triplet and the density near Earth's center, Science, 255, 1678-1682; doi:10.1126/science.255.5052.1678.

Tanimoto, T. (1990). Lateral variation of Q from singlet modal Q measurements of ${}_0S_2$, Geophys. Res. Lett., 17 (6), 669-672; doi:10.1029/GL017i006p00669.

Taylor, J.R. (1997). An Introduction to Error Analysis: The Study of Uncertainties in Physical Measurements, University Science Books, 327 pp.

Tromp, J., and E. Zanzerkia (1995). Toroidal splitting observations from the great 1994 Bolivia and Kuril Islands earthquakes, Geophys. Res. Lett., 22, 16, 2297-2300.

Widmer-Schnidrig, R., G. Masters and F. Gilbert (1992a). Observably split multiplets-data analysis and interpretation in terms of large-scale aspherical structure, Geophys. J. Int., 111, 559-576; doi:10.1111/j.13 65-246X.1992.tb02112.x.

Widmer-Schnidrig, R., W. Zürn and G. Masters (1992b). Observation of low-order toroidal modes from the 1989 Macquarie Rise event, Geophys. J. Int., 111, 226-236.

Widmer-Schnidrig, R. (2003). What can superconducting gravimeters contribute to normal mode seismology?, Bull. Seismol. Soc. Am., 93 (3), 1370-1380; doi:10.1785/0120020149.

Widmer-Schnidrig, R., and G. Laske (2007). Theory and observations – normal modes and surface wave measurements, In: B.A. Romanowicz and A.M. Dziewonski (eds.), Treatise on Geophysics, Vol.1: Seismology and the Structure of the Earth. Elsevier, Amsterdam, The Netherlands, 67-125.

Xu, Y., D. Crossley and R.B. Herrmann (2008). Amplitude and Q of ${}_0S_0$ from the Sumatra earthquake as recorded on superconducting gravimeters and seismometers, Seismol. Res. Lett., 79 (6), 797-805; doi: 10.1785/gssrl.79.6.797.

Zábranová, E., C. Matyska, L. Hanyk and V. Pálinkáš (2012). Constraints on the centroid moment tensors of the 2010 Maule and 2011 Tohoku earthquakes from radial modes, Geophys. Res. Lett., 39, L18302; doi:10.1029/2012GL052850.

*Corresponding author: WenBin Shen,
Wuhan University, Department of Geophysics, School of Geodesy and Geomatics, China; email: wbshen@sgg.whu.edu.cn.